remote sensing

MDPI

Article

Vertical Characteristics of Vegetation Distribution in Wuyishan National Park Based on Multi-Source High-Resolution Remotely Sensed Data

Yongpeng Ye [1,2], Dengsheng Lu [1,2], Zuohang Wu [3], Kuo Liao [3], Mingxing Zhou [1,2], Kai Jian [1,2] and Dengqiu Li [1,2,*]

[1] Fujian Provincial Key Laboratory for Subtropical Resources and Environment, Fujian Normal University, Fuzhou 350117, China; qsx20211164@student.fjnu.edu.cn (Y.Y.)
[2] Institute of Geography, Fujian Normal University, Fuzhou 350007, China
[3] Fujian Institute of Meteorological Science, Fuzhou 350001, China
[*] Correspondence: lidengqiu@fjnu.edu.cn

Abstract: Identifying vertical characteristics of mountainous vegetation distribution is necessary for studying the ecological environment quality and biodiversity and for evaluating its responses to climate change. However, producing fine vegetation distribution in a complex mountainous area remains a huge challenge. This study developed a framework based on multi-source high-resolution satellite images to strengthen the understanding of vertical features of vegetation distribution. We fused GaoFen-6 and Sentinel-2 data to produce 2 m multispectral data, combined with ALOS PALSAR digital elevation model (DEM) data, and used an object-based method to extract variables for establishing a classification model. The spatial distribution of vegetation types in Wuyishan National Park (WNP) was then obtained using a hierarchical random forest classifier. The characteristics of different vegetation types along the elevation gradient and their distribution patterns under different human protection levels were finally examined. The results show that (1) An overall accuracy of 87.11% and a Kappa coefficient of 0.85 for vegetation classification was achieved. (2) WNP exhibits obviously vertical differentiation of vegetation types, showing four compound dominant zone groups and five dominant belts. (3) The composition of vegetation types in the scenic area differs significantly from other regions. The proportions of Masson pine and Chinese fir exhibit a noticeably decreasing trend as the distance increases away from roads, while the changes in broadleaf forest and bamboo forest are less pronounced.

Keywords: Wuyishan National Park; multi-source high-resolution remote sensing; vegetation types; vertical gradient

check for updates

Citation: Ye, Y.; Lu, D.; Wu, Z.; Liao, K.; Zhou, M.; Jian, K.; Li, D. Vertical Characteristics of Vegetation Distribution in Wuyishan National Park Based on Multi-Source High-Resolution Remotely Sensed Data. *Remote Sens.* **2023**, *15*, 5023. https://doi.org/10.3390/rs15205023

Academic Editors: Bogdan Andrei Mihai and Marcel Torok

Received: 26 September 2023
Revised: 16 October 2023
Accepted: 17 October 2023
Published: 19 October 2023

1. Introduction

Mountains condense the physical geography and ecology of horizontal natural zones due to their significant environmental gradients within a relatively small spatial range [1,2]. The altitudinal spectrum of these gradients serves as a critical indicator of climate change and amplifies the signals of climate variations [3,4]. Accurately describing the vertical zones of mountainous vegetation types is an effective approach to unravel the complexities and heterogeneity of mountain environments. National parks, often situated in complex mountainous regions, preserve pristine natural habitats with limited human interference. They exhibit distinct vertical vegetation zones, serving as havens for biodiversity and showcasing key ecological processes [5], and become the focus area for examining altitudinal belts of vegetation types.

The traditional way of revealing the distribution patterns along the altitude gradient of mountainous vegetation is through field surveys using random sampling or continuous transects in representative communities. It is conducive to further analyze vegetation composition and structure, altitudinal belts spectrum, species diversity, and their relationships with environmental factors [6,7]. A field survey method can provide accurate species details but exhibits low spatiotemporal continuity and requires substantial human resources. Few field samples or transects used to represent the boundary of vegetation distribution within the vertical zones weaken the transitional characteristics of vertical boundaries and increase the uncertainty in quantitative analysis of mountainous vegetation spectrum structure evolution [8]. In addition, previous research primarily focused on the delineation of vertical boundaries for individual or few vegetation types (such as tree-line, snowline), resulting in a very limited knowledge of the altitudinal belts across the mountains [9,10].

Remote sensing data have the advantage of wide coverage, long time series, and low cost. With the improvement of spatial, temporal, and spectral resolutions, it provides an effective solution for accurate vegetation classification and altitudinal belt analysis [11–13]. However, previous studies often relied on medium- or low-resolution remote sensing data [12,14], treating forests as one category [8]. While this might be suitable for areas with large elevation differences, complex and diverse habitats, and varied land cover types (such as in the Qinghai–Tibet Plateau), it cannot capture the altitudinal spectrum in mountainous zones where different vegetation types are transformed within forests. Some remote sensing-based land cover products have subdivided forests into finer categories, such as evergreen broadleaf forest, deciduous broadleaf forest, and evergreen coniferous forest, improving the ability to characterize mountainous vegetation altitudinal belts. However, for subtropical forest ecosystems with complex and diverse tree species, their ability to identify land cover types is extremely limited. Taking the GLC_FCS30 product as an example, it includes only three forest categories in the Wuyishan region: open evergreen broadleaf forest, closed deciduous broadleaf forest, and closed evergreen coniferous forest [15]. Therefore, it is necessary to utilize high-resolution remote sensing data to better reveal the altitudinal belt characteristics of vegetation in typical subtropical mountainous areas.

The development of high-resolution remote sensing technology and the availability of high spatial resolution remote sensing data (such as Quickbird, Worldview, ZiYuan, and GaoFen (GF) satellites) have provided new opportunities for vegetation mapping and altitudinal belt analysis [16–18]. High spatial resolution imagery enhances the ability to capture fine-grained surface features but exacerbates the spectral heterogeneity within objects, leading to the "salt-and-pepper" effect in pixel-based classification methods. This issue can be effectively addressed by segmenting the imagery into homogeneous objects, resulting in higher classification accuracy [19–22]. It is crucial to select appropriate variables avoiding the "curse of dimensionality" [23,24]. When dealing with a limited number of variables, parametric classifiers such as maximum likelihood can be used for vegetation classification [25]. Machine learning algorithms can achieve higher classification accuracy when dealing with complex data with high-dimensional features [26–28]. However, research on multi-source high-resolution remote sensing data for land cover classification at the scale of national parks is still limited. The development of high-resolution remote sensing technology raises the question of whether it can improve our understanding of the complex altitudinal spectrum in mountainous areas, which is a topic of common concern in remote sensing technology and ecological research.

Wuyishan National Park (WNP) is in the subtropical region of China with large elevation variation. It possesses unique natural habitat conditions, preserving the zonal vegetation of the central subtropical evergreen broadleaf forest. It also exhibits a significant vertical gradient, with various vegetation types distributed from low to high elevations, including evergreen broadleaf forest, mixed coniferous and broadleaf forest, coniferous forest, and meadow. As a dual World Cultural and Natural Heritage site, WNP has different levels of protected and utilized regions, resulting in complex ecosystem types and altitudinal differentiation. Currently, research on the vertical gradient of vegetation in WNP is mostly based on field investigations, focusing on the composition, structure, and biodiversity of specific vegetation communities [29]. Most of these studies were conducted several decades ago and lack spatially continuous distribution information [30,31]. Remote sensing-based research in WNP primarily focuses on vegetation cover, landscape pattern analysis, ecological quality assessment [32], and the utilization of time series data for analyzing spatial patterns of vegetation changes and monitoring treeline dynamics in response to climate change [33–35]. The spatially continuous distribution characteristics of vegetation types along the vertical gradient in WNP are yet to be investigated. This study integrates GF-6 and Sentinel-2 images, uses an object-based hierarchical random forest classifier for vegetation mapping in WNP, and identifies the vertical distribution pattern of each vegetation type. Specifically, our main objective is to explore the vertical distribution patterns of vegetation types in WNP, assess the significance of differences in vertical distribution patterns among different vegetation types, and investigate the impact of human protections on the vertical characteristics of vegetation distribution.

2. Study Area

WNP is located in the northern part of Fujian Province (Figure 1a). The area is 1001.41 km^2 and the elevation ranges from 171 m to 2161 m. This region has a typical subtropical monsoon climate with average annual temperature of 18 °C and annual precipitation of 1684–1780 mm. A total of 2799 plant species have been recorded in this park [36]. Besides the typical zonal evergreen broadleaf forest, this park also features warm temperate coniferous forest, subtropical coniferous forest, mixed forest, bamboo forest, shrub, grass, and meadows.

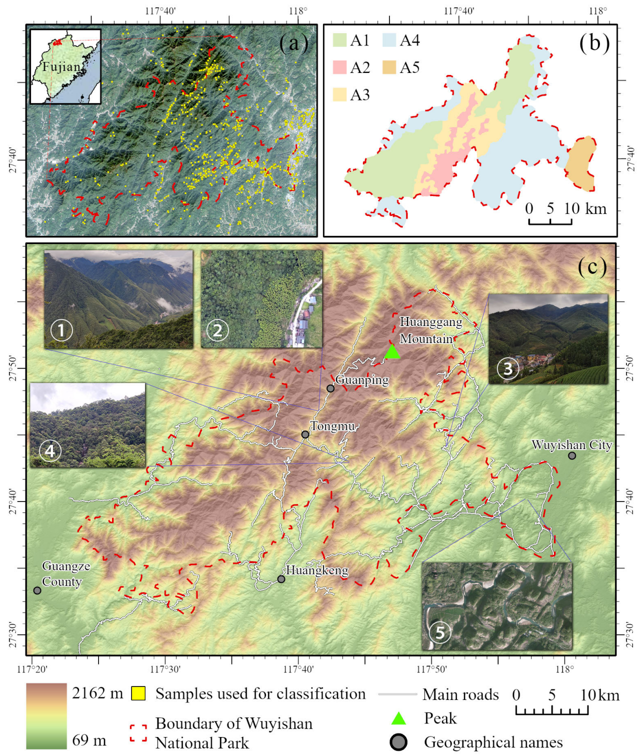

Figure 1. The location of WNP and samples used for classification (background image: Sentinel-2, composite bands: R: Band 4, G: Band 3, B: Band 2) (**a**), the boundaries of different subregions within the park (**b**), and main roads, peaks, and associated geographical names with DEM (**c**). Plots ①–⑤ show the vegetation in different areas and at different elevations captured using drones and smartphones. Plots ① and ② depict the distribution of broadleaf and bamboo forests on slopes near roads and residential areas. Plot ③ captures broadleaf forests, while Plot ④ showcases Chinese fir and tea plantations, providing a comparison of vegetation landscapes in different subregions at similar elevation. Plot ⑤ visually presents the unique vegetation distribution in the scenic area, clearly showing the presence of tea plantations and non-vegetated areas (bare rocks and mudflats), among others.

The northwest region of WNP was established as the National Nature Reserve in 1979 and the southeast region was established as scenic area in 1982. Both combined areas were successfully listed as a World Natural and Cultural Heritage site in 1999. In 2021, WNP was designated as one of the initial batches of national parks established in China. Based on the historical evolution of protective measures and research contents, WNP was divided into five subregions (Figure 1b), with variations in protective measures as shown in Table 1.

Table 1. Five subregions under different protection measures in Wuyishan National Park.

Code	Regions	Protection Measures	Area (km^2)	Elevation Range (m)	Average Elevation (m)	Standard Deviation of Elevation (m)
A1	Core Area of Nature Reserve	Strict protection, only allowing scientific research activities	329.05	297–2155	1175.65	359.30
A2	Experimental Area of Nature Reserve	Strict protection, only allowing scientific research, teaching internships, and similar activities	89.06	404–1655	915.50	232.28
A3	Buffer Area of Nature Reserve	Strict control, allowing scientific experiments, teaching internships, tourism, and similar activities	159.85	421–1927	1190.60	310.68
A4	Ecological Protection Area	Strict control, allowing ecological restoration and scientific research and education, with limited tourism development	424.14	200–1864	812.20	325.29
A5	Scenic Area	General, allowing planned production activities and infrastructure construction that comply with regulations	64.09	171–724	288.67	89.20

3. Data and Methods

The framework of this study consisted of three main parts (Figure 2): (1) Data acquisition and collection; (2) Fine classification of vegetation types based on GF-6 panchromatic band and Sentinel-2 multispectral bands; (3) Analysis of altitudinal belts of vegetation types in WNP.

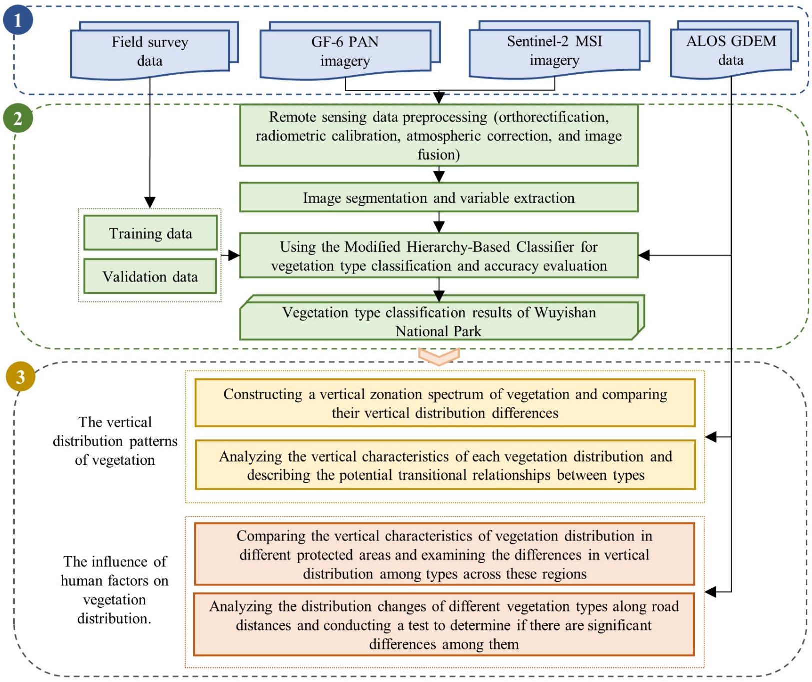

Figure 2. Framework for studying the vertical characteristics of vegetation distribution in Wuyishan National Park (GF-6, PAN, and MSI indicate GaoFen-6, panchromatic, and multispectral instrument, respectively).

3.1. Dataset and Preprocessing

3.1.1. Sample Data Collection and Classification System Design

A total of 957 samples were collected through field surveys in April and August 2021. We collected the samples by drawing polygons on the fused images of GF-6 and Sentinel-2 and Google Earth based the vegetation type labels from the field surveys. All the samples used to train and test the classification model are in polygon forms. The classification system was designed with a total of 11 vegetation categories, including Masson pine (*Pinus massoniana*) (60 samples), Chinese fir (*Cunninghamia lanceolata*) (117 samples), other coniferous forests (53 samples), mixed coniferous and broadleaf forest (80 samples), broadleaf forest (73 samples), bamboo forest (119 samples), shrubland (11 samples), grassland (11 samples), farmland (110 samples), tea plantation (102 samples), and non-vegetated lands (221 samples). There are very limited areas of grassland and shrubland in WNP and few samples were collected. Masson pine and Chinese fir are the main timber tree species in southern China and are distributed in and around WNP. Other coniferous forests mainly include southern hemlock (*Tsuga chinensis* var. *tchekiangensis*) and Huangshan pine (*Pinus hwangshanensis*). Broadleaf forest mainly includes Castanopsis eyrei (*Castanopsis eyrei*), Castanopsis carlesii (*Castanopsis carlesii*), Schima superba (*Schima superba*), and other broadleaf tree species widely distributed in WNP. Bamboo forest includes Moso bamboo (*Phyllostachys edulis*), dwarf bamboo (*Oligostachyum oedogonatum*), and Yushan bamboo (*Yushania wuyishanensis*). Shrub mainly grows in areas with poor site conditions or at higher altitudes. Grassland mainly includes artificially managed grasslands and natural grasslands. Farmland includes cultivated land with crops and fallow land. Non-vegetated mainly includes tidal flats, rocks, bare soils, impervious surface areas, and water bodies. These samples were divided into training and validation sets using stratified random sampling with a ratio of 6:4.

3.1.2. Collection and Preprocessing of Remotely Sensed Data

The study area experiences frequent cloud cover and rainfall, making it difficult to obtain high-quality optical sensor imagery that matches the time of the field surveys. We collected GF-6 and Sentinel-2 images, and ALOS PALSAR DEM (Table 2). The vegetation types in the study area are relatively stable between field survey and remote sensing data. The GF-6 panchromatic (PAN) band has a spatial resolution of 2 m, and four bands of Sentinel-2 L1C products have a spatial resolution of 10 m, while the remaining bands with 20 m were resampled to the same spatial resolution using the Sen2Res method [37]. Several preprocessing steps including orthorectification, radiometric calibration, and atmospheric correction were performed. The Gram–Schmidt method [38] was used to integrate Sentinel-2 multispectral bands and GF-6 PAN band to gain improved spatial resolution of multispectral bands.

Table 2. Main data sources and related information.

	Data Source	Spatial Resolution	Acquire Time
High-resolution data	GF-6	Panchromatic band: 2 m	22 November 2019
Multispectral data	Sentinel-2	Blue, Green, Red, NIR bands: 10 m Other bands used: 20 m	13 December 2019
Terrain data	ALOS PALSAR DEM	12.5 m	\

3.2. Vegetation Classification Based on the Fused Remotely Sensed Data

When high spatial resolution images were used for vegetation classification, previous research has indicated that the object-based classification methods performed better than pixel-based methods [39]. The segmentation was performed using the multi-resolution segmentation algorithm in eCognition software (version 9.0.1). The segmentation parameters were determined through iterative experiments and finally set as follows: scale parameter of 250, shape of 0.1, and compactness of 0.5. A total of 4,151,112 objects were obtained with an average area of 660.72 m^2. A total of 26 variables were extracted based on the segmentation objects, including spectral bands from the fused image (10 bands); texture variables computed from the gray-level co-occurrence matrix (GLCM) (homogeneity, contrast, dissimilarity, entropy, angular second moment, mean, standard deviation, correlation); geometric features calculated from the segmentation objects (length/width, asymmetry, compactness, density, shape index);and elevation, slope, and aspect derived from ALOS PALSAR DEM data.

Too many variables used for vegetation classification cannot guarantee an improved classification performance, especially in the complex landscapes under investigation and insufficient training samples. Therefore, it is necessary to optimize the feature set for different vegetation types. We adopted a modified hierarchy classifier based on an automated optimization of tree structure and variables using the Z-score algorithm [40]. A cyclic iteration process was employed to obtain the optimal set of variables for each hierarchical node. In comparison to the overall optimal variable selection approach of random forest, the hierarchy method selects the optimal variable combinations for each hierarchical node. The classification result was evaluated using overall accuracy, Kappa coefficient, producer's accuracy (PA), and user's accuracy (UA).

3.3. Characterizing Distribution Patterns of Vegetation Types

3.3.1. Vertical Distribution Patterns of Vegetation Types

The areal proportions of different vegetation types were extracted at various elevations, constructing a vertical gradient of vegetation types. Considering the disparity of spatial resolution between the ALOS PALSAR DEM data (12.5 m) and the vegetation classification results (2 m), the elevation range was divided into 50 m intervals, named as vertical zones, and the areal proportions of vegetation types within each 50 m zone were calculated to obtain the altitudinal belts of vegetation types. The difference test was used to evaluate the vertical distribution differences among vegetation types. The Wilcoxon signed-rank test was employed to examine the statistical significance considering its ability to tackle the abnormal data distribution [7]. The calculated cumulative sums of areal proportions with vertical zones were used for a difference significance test to ensure consistency between the orders of altitudinal belts for each vegetation type.

Based on previous research [8], the distribution of upper/lower limits, core distribution zone, main distribution zone, dominant belt, and compound dominant zone (Table 3) were adopted to describe the vertical structure and composition characteristics of vegetation types. By examining the relationships within the dominant belt, compound dominant zone, and compound dominant zone group (combination of adjacent compound dominant zones), the internal relationships of the vegetation altitudinal belts were elucidated. Additionally, compound dominant zones and compound dominant zone groups were named based on their elevation ranges (e.g., low-elevation compound dominant zone group, high-elevation compound dominant zone) to succinctly express potentially transitional relationships among vegetation types in the altitudinal belts spectrum.

Table 3. Definitions of terminology for describing vertical distribution of vegetation types.

Terms	Definitions	Determination Method
Distribution of Upper/Lower Limits	The elevation at the highest and lowest zones where a vegetation type exhibits continuous distribution.	The highest elevation where the type appears within a zone represents the upper limit, whereas the lowest elevation represents the lower limit of the distribution for that type.

Table 3. *Cont.*

Terms	Definitions	Determination Method
Core Distribution Zone	The number of vertical zones occupied by the type is less than one-third of the total number of vertical zones within its distribution range, and the areal proportion of the type's distribution within these zones is more than two-thirds of the total distribution area for that type.	Starting from the elevation zone with the highest proportion of the vegetation type's area, the core distribution zone extends equally in both directions (upward and downward) in terms of area ratio. When the cumulative areal proportion of the type reaches more than two-thirds, the vertical distribution range is defined as the core zone (core distribution range) for that type. The number of vertical zones within the core zone should be less than one-third of the total number of vertical zones occupied by the type.
Main Distribution Zone	The vertical zones where the vertical distribution area of the vegetation type accounts for more than two-thirds of the total area of that type while lacking core distribution zone within its vertical distribution range.	Starting from the vertical zone with the highest proportion of the vegetation type's area, the main distribution zone extends equally in both directions (upward and downward) based on area ratio. When the cumulative areal proportion of the type reaches more than two-thirds, the vertical distribution range of that type is defined as the main distribution range.
Dominant Belt	One vegetation type accounts for more than two-thirds of the zone's area.	The proportion of a specific vegetation type's distribution area within a vertical zone exceeds two-thirds of that zone's area.
Compound Dominant Zone	It is characterized by two or more vegetation types, with the name based on the proportion of their respective distribution areas.	No single vegetation type dominates a vertical zone (the proportion does not reach more than two-thirds of the area). Vegetation types with a combined proportion exceeding two-thirds are selected in descending order based on their areal proportions, and the zone is named after these dominant types.

3.3.2. Impact of Human Factors on Vegetation Type Distribution

Protection measures are important indicators for quantifying human disturbances to vegetation. We examined the differences of vegetation vertical distributions among five distinct areas under different protective measures (Table 1). The proportion cumulative sum of each vegetation type's area in each subregion was calculated and the significance of their differences was calculated using the Wilcoxon signed-rank test. In addition, we performed separate tests for each vegetation type's areal proportion across vertical zones in each region to reveal the differences in vertical distribution patterns of various vegetation types within different levels of protected areas.

Although the five subregions are all under protection, human activities related to production and livelihood (such as tree planting and logging, cultivation of farmland and tea plantation, and expansion of construction areas) can lead to changes in vegetation types. These activities can alter the spatial and vertical distribution of vegetation types. Considering these human activities are closely related to the roads, we utilized OpenStreetMap data and remote sensing imagery to produce a major roads map of WNP (Figure 1c). The Euclidean distance between each pixel within WNP and the nearest road was calculated, resulting in the spatial distribution of the nearest road distance. To ensure relative consistency in the number of pixels between different intervals, the road distance was reclassified using a quantile method. The proportions' cumulative sum of different vegetation types within road distance intervals were then statistically analyzed using the

Wilcoxon signed-rank test, to determine whether there were significant differences across road distance intervals.

4. Results

4.1. Analysis of Classification Results

The error matrix (Table 4) shows that an overall classification accuracy of 87.11% with a Kappa coefficient of 0.85 was obtained. The highest classification accuracy was for other coniferous forests and non-vegetated lands, while the lowest accuracy was for mixed coniferous and broadleaf forest. Confusion mainly occurs among Masson pine, Chinese fir, other coniferous forests, and mixed coniferous and broadleaf forest. The accuracy of bamboo forest was relatively high, with both PA and UA exceeding 91%.

Table 4. Classification accuracy and area statistics for each vegetation type.

	MP	**CF**	**OC**	**MCB**	**BL**	**BB**	**SL**	**GL**	**FL**	**TP**	**NV**	**Total**
MP	17			2								19
CF	1	43		2	4					2		52
OC	1		21									22
MCB	3	2	1	21	1					1		29
BL	1	1		5	24	2				2		35
BB				1	1	44				2		48
SL							4				1	5
GL								3				3
FL									40	1	1	42
TP	1	1				2	1		2	33		40
NV								2	3		88	93
Total	24	47	22	31	30	48	5	5	45	41	90	388
PA (%)	70.8	91.5	95.5	67.7	80.0	91.7	80.0	60.0	88.9	80.5	97.8	
UA (%)	89.5	82.7	95.5	72.4	68.6	91.7	80.0	100.0	95.2	82.5	94.6	
Area (km^2)	12.8	60.3	50.8	265.5	435.0	156.4	1.1	0.3	7.0	53.2	23.9	
Area Percentage (%)	1.2	5.7	4.8	24.9	40.8	14.7	0.1	0.03	0.7	5.0	2.3	

Notes: MP: Masson pine; CF: Chinese fir; OC: Other coniferous forests; MCB: Mixed coniferous and broadleaf forest; BL: Broadleaf forest; BB: Bamboo forest; SL: Shrubland; GL: Grassland; FL: Farmland; TP: Tea plantation; NV: Non-vegetated lands.

Analysis of the classification result (Figure 3) indicates that forest area accounts for 91% of the national park area, with broadleaf forest, mixed coniferous and broadleaf forest, and bamboo forest the dominant forest types. The vegetation types relating to human activities (such as Masson pine, Chinese fir, farmland, and tea plantation) accounts for approximately 12.5% of the total park area. Non-vegetated areas account for approximately 2.25% of the total area. Masson pine and Chinese fir are mainly located in the southeastern part of the national park, while other coniferous forests are found in the western and northern parts of the park. Mixed coniferous and broadleaf forest, broadleaf forest, and bamboo forest are widely distributed throughout the entire national park. Farmland and tea plantation are mainly concentrated on both sides of the main road. Non-vegetated areas are mainly located at high-elevation mountain tops and steep cliffs, as well as internal roads and residential areas. Shrubland and grassland are relatively scarce and sparsely distributed within the national park.

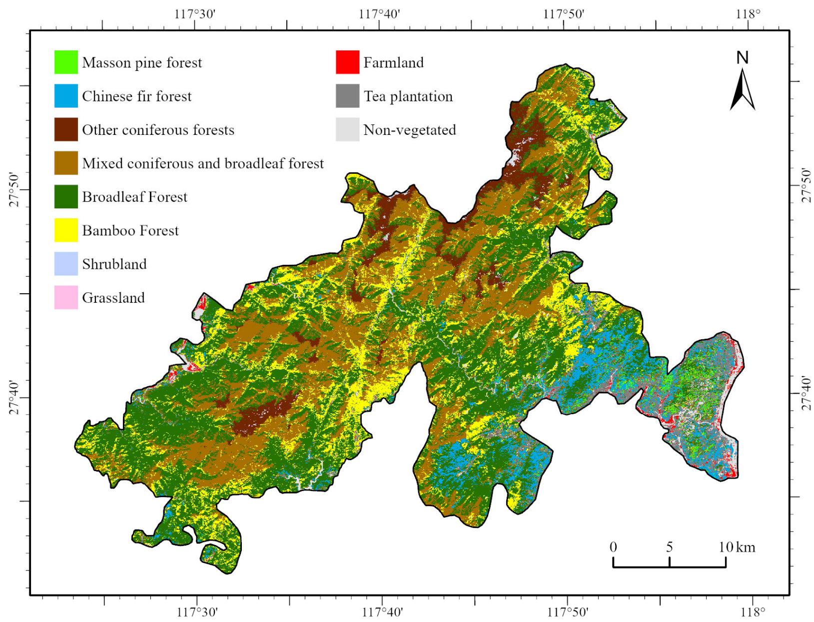

Figure 3. Spatial distribution of vegetation types in Wuyishan National Park.

4.2. Vertical Characteristics of Vegetation Distribution in Wuyishan National Park

The distribution of Masson pine and Chinese fir extends over a wide range of altitudes, but primarily in the low-elevation zones (200–500 m and 200–600 m). Other coniferous species are mainly distributed in the range of 1300–1750 m, exhibiting higher main distribution zone and narrower vertical distribution range than Masson pine and Chinese fir (Figure 4 and Table 5). Mixed coniferous and broadleaf forest, broadleaf forest, and bamboo forest have similar vertical distribution ranges. However, the main distribution zone of mixed coniferous and broadleaf forest (200–1400 m) has a higher upper boundary than the other two vegetation types (200–1000 m, 200–1050 m). The mixed coniferous and broadleaf forest exhibits two peaks around the 500 m and 1400 m zones (Figure 4).

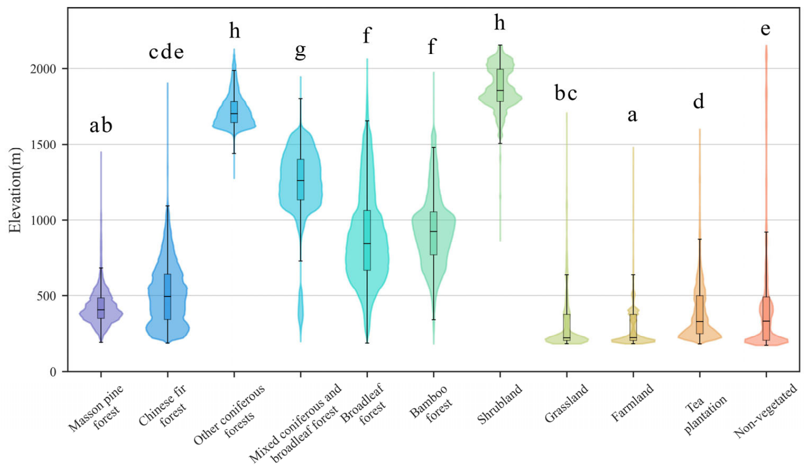

Figure 4. The vertical distribution range and significance of differences in the distribution patterns among vegetation types. (Significances of differences between vegetation types in vertical distribution patterns are represented by labeling letters. If the labels of two vegetation types contain any of the same letter, it indicates a non-significant difference between the two vegetation types; otherwise, a significant difference exists between the two vegetation types in the vertical distribution. For example, the difference test between Masson pine and Chinese fir is significant, because they do not share the same letter, but it is non-significant between Masson pine and grassland, since they share the same letter b.)

Table 5. The vertical distribution range and core and main distribution zones for each vegetation type.

Vegetation Types	Distribution Upper/Lower Limits (m)	Core Distribution Zone (m)	Main Distribution Zone (m)
Masson pine	200–1450	/	200–500
Chinese fir	200–1950	/	200–600
Other coniferous forests	1300–2150	/	1300–1750
Mixed coniferous and broadleaf forest	200–1950	/	200–1400
Broadleaf forest	200–1950	/	200–1000
Bamboo forest	200–2000	/	200–1050
Shrubland	900–2200	/	2150–2200
Grassland	200–1750	200–300	/
Farmland	200–1650	200–350	/
Tea plantation	200–1750	/	200–450
Non-vegetated lands	200–2200	/	200–450

Non-forest vegetation types exhibit distinct polarization in their vertical distribution. Shrubland is predominantly concentrated in high-altitude areas, with the core distribution zone (2150–2200 m) spatially corresponding to the summit area of Huanggang Mountain (the highest peak in WNP). Grassland, farmland, and tea plantation share a similar vertical distribution range. Grassland and farmland have core distribution zones (200–300 m, 200–350 m) concentrated in low-altitude areas, while tea plantation has a higher and more dispersed distribution range, with the main distribution zone at 200–450 m. Non-vegetated area shows the widest range of vertical distribution (spanning across all vertical zones), with the main distribution zone concentrated in low-altitude areas (200–450 m).

The Wilcoxon signed-rank test showed that there are significant differences in the vertical distribution between coniferous forest types and broadleaf forest, and both Masson pine, Chinese fir, and other coniferous forests exhibit significant differences in vertical distribution range (Table 5) and distribution patterns (Figure 4) compared to broadleaf forest and bamboo forest. The three coniferous forest types, Masson pine, fir, and other coniferous forests, also show significant differences in distribution between them. Other coniferous forests show non-significant differences compared to shrubland. Farmland, tea plantation, and non-vegetated, which are directly influenced by human activities, demonstrate significant differences in their vertical distribution patterns compared to species such as other coniferous forests, mixed coniferous and broadleaf forest, broadleaf forest, and bamboo forest. However, their vertical distribution patterns do not significantly differ from those of Masson pine and Chinese fir.

There are transitional zones among different vegetation types along the vertical gradient according to the dominant belts and compound dominant zones (Table 5 and Figure 5). The transitional zones are observed in the entire vertical gradient, with four compound dominant zones and five dominant belts appearing alternatively. There is an obvious transitional relationship among vegetation types within the compound dominant zone groups. In the low-elevation range of 200–600 m, the compound dominant zone is dominated by non-vegetated areas, farmland, tea plantation, Chinese fir forest, and broadleaf forest in sequence. In the mid-elevation range (900–1350 m), a compound dominant zone appears with a dominance of broadleaf forest, bamboo forest, and mixed coniferous and broadleaf forest. In the mid-high elevation range (1550–1600 m), a compound dominant zone emerges with a dominance of mixed coniferous and broadleaf forest, broadleaf forest, and other coniferous forests.

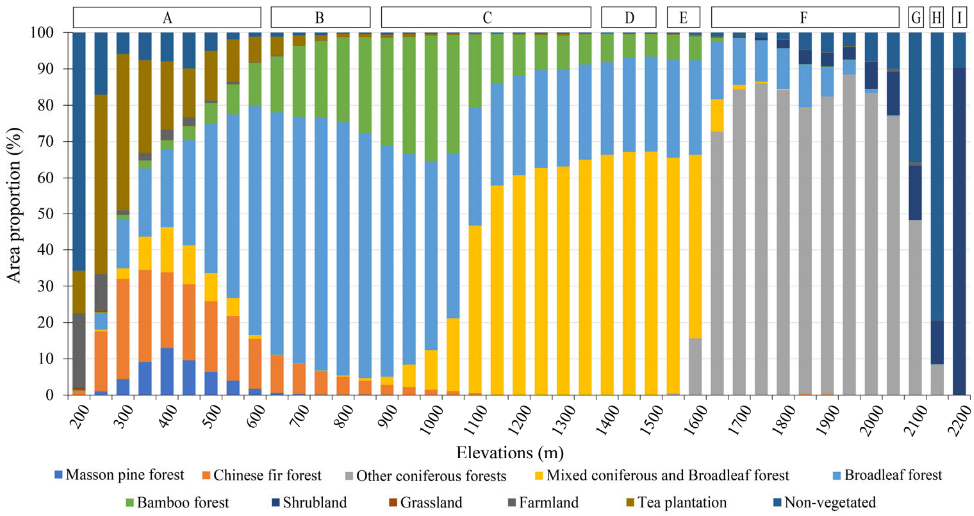

Figure 5. The areal proportion of each vegetation type in different vertical zones, and compound dominant zones and altitudinal belts (represented by letters as follows: A: low-elevation compound dominant zone group; B: dominant belt of broadleaf forest; C: mid-elevation compound dominant zone group; D: dominant belt of mixed coniferous and broadleaf forest; E: mid-high elevation compound dominant zone group; F: dominant belt of other coniferous forests; G: high-elevation compound dominant zone; H: dominant belt of non-vegetated areas; I: dominant belt of shrubland).

4.3. Influence of Human Factors on the Vertical Characteristics of Vegetation Distribution

4.3.1. Vegetation Distribution in Five Subregions under Different Protection Levels

There are differences in the proportions of vegetation types among the five subregions (Table 6), but none of them reach a significant difference. The dominant vegetation types in the Nature Reserve (including core area, experimental area, and buffer area) are other coniferous forests, mixed coniferous and broadleaf forest, broadleaf forest, and bamboo forest. The core area and buffer area have similar areal proportions of vegetation types, but the experimental area has a significantly higher proportion of bamboo forest and tea plantation. The proportions of Chinese fir and tea plantation increase successively from the Nature Reserve to the ecological protection area and scenic area. The vegetation composition in the scenic area differs from other regions, with a higher proportion of Masson pine, Chinese fir, tea plantation, and non-vegetated area.

Table 6. Areal proportions of vegetation types in five subregions of Wuyishan National Park (%).

	MP	CF	OC	MCB	BL	BB	SL	GL	FL	TP	NV
Core Area (A1)	0.14	0.30	10.62	33.14	43.19	10.60	0.23	0.00	0.18	0.75	0.86
Experimental Area (A2)	0.04	0.44	7.22	41.92	35.97	12.58	0.17	0.00	0.03	0.80	0.82
Buffer Area (A3)	0.14	1.43	0.06	21.77	37.66	33.96	-	0.01	0.09	3.06	1.82
Ecological Protection Area (A4)	1.52	10.80	1.01	15.91	45.41	16.57	0.01	0.03	0.65	6.33	1.75
Scenic Area (A5)	8.94	17.95	-	3.94	14.32	1.33	-	0.24	5.48	31.01	16.78

Notes: MP: Masson pine; CF: Chinese fir; OC: Other coniferous forests; MCB: Mixed coniferous and broadleaf forest; BL: Broadleaf forest; BB: Bamboo forest; SL: Shrubland; GL: Grassland; FL: Farmland; TP: Tea plantation; NV: Non-vegetated.

The Wilcoxon signed-rank test on the cumulative sum of areal proportion for each subregion showed that the five subregions exhibit variations in the vertical distribution of each vegetation type, with a total of 83 significant difference in all vegetation types and regions. There are discrepancies in the cumulative frequency of vertical distribution differences among the five subregions (Figure 6). The scenic area exhibits the largest differences in vertical distribution patterns and shows significant differences in 36 instances across nine vegetation types. The core area, experimental area, and ecological protection area have 34, 35, and 33 instances of significant differences, respectively, and the buffer area has 28 instances of significant differences. Vegetation types also exhibit varying frequencies of significant differences among different regions. Masson pine shows no significant difference among the five subregions, representing the category with the lowest frequency of distinct differences of vertical distributions.

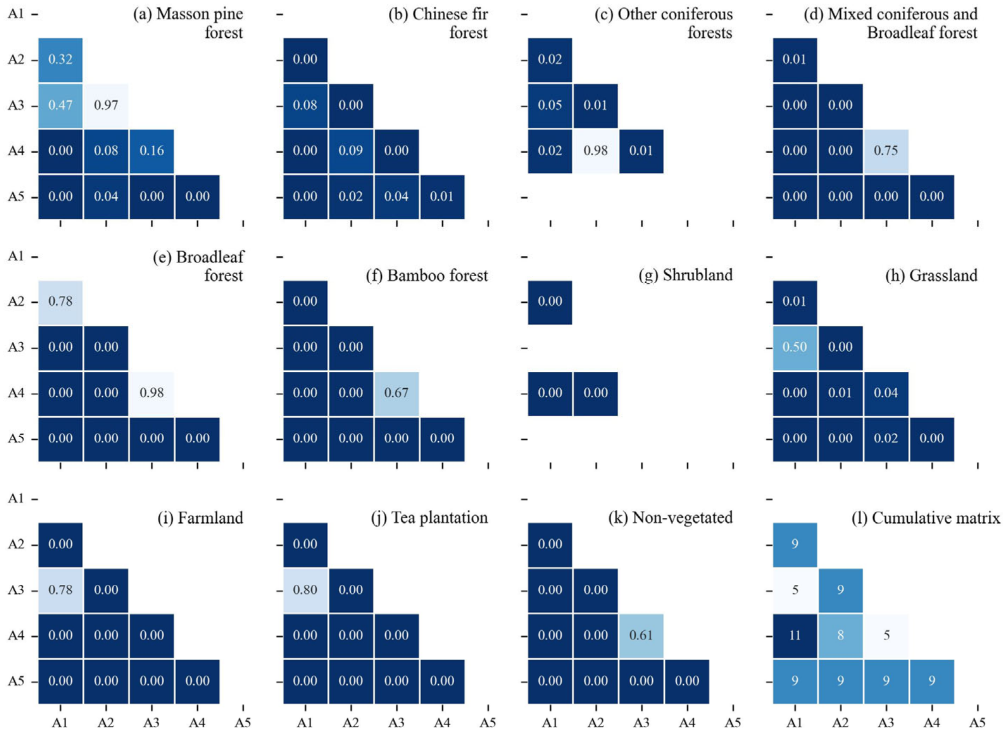

Figure 6. Significant analysis results of vertical distribution differences among different vegetation types in regions of different protection levels (**a**–**k** represent the *p*-values of significant analysis for each type; subplot **l** represents the cumulative matrix of significant differences, which is the cumulative number of significant differences in the test results displayed in **a**–**k**). A1–A5 represent five regions: A1: Core Area of Nature Reserve; A2: Experimental Area of Nature Reserve; A3: Buffer Area of Nature Reserve; A4: Ecological Protection Area; A5: Scenic Area.

4.3.2. Vegetation Distribution with Road Distance

The proportion of each vegetation type varies with road distance increases, and there are differences in the sequence of changes in proportion among different types (Figure 7). The areas of Masson pine and Chinese fir show a decreasing trend with increasing road distance. The proportions of broadleaf forest and bamboo forest show little change along the road distance. Mixed coniferous and broadleaf forest, as well as other coniferous forests, exhibit significant changes in proportions across different intervals, but they do not show a clear gradient with increasing road distance. The areal proportions of all non-forest types (such as grassland, farmland, tea plantation, and non-vegetated areas) show a decreasing trend with increasing road distance. There are significant differences in the trends between most types ($p < 0.05$), except for the pairs of Masson pine—Chinese fir, Masson pine—non-vegetated, Chinese fir—non-vegetated, grassland—farmland, and tea plantation—non-vegetated (Figure 7).

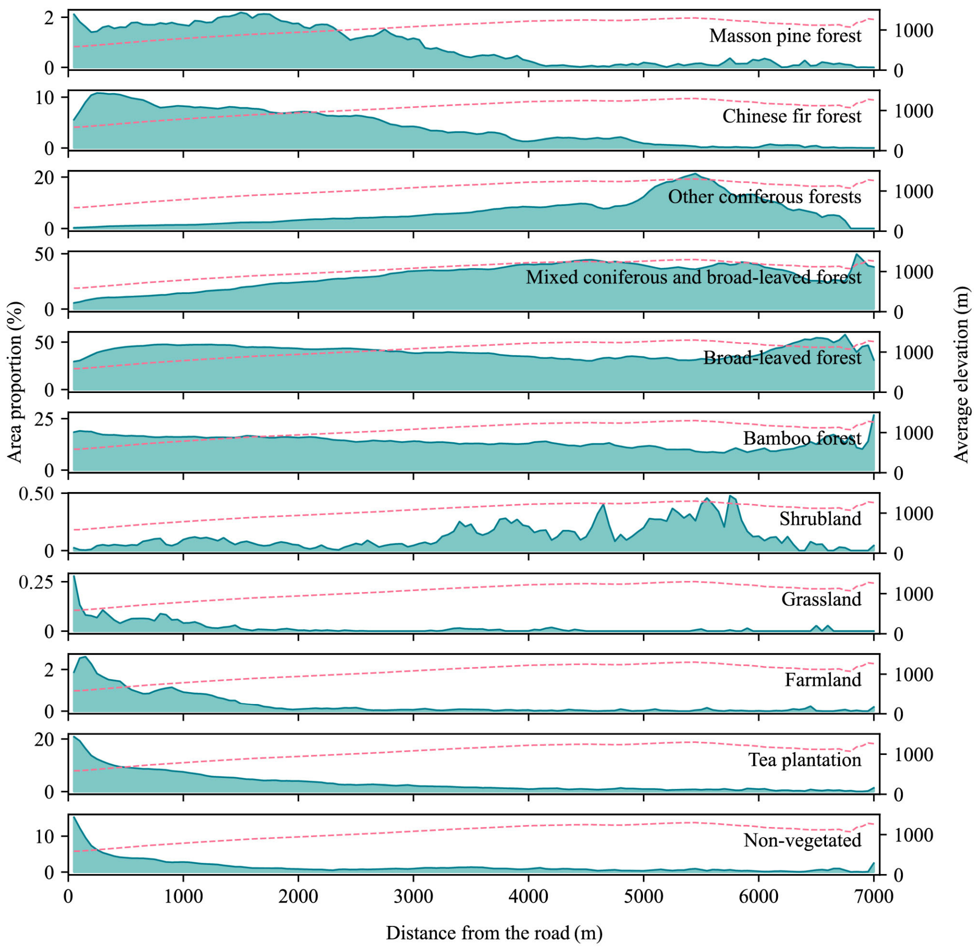

Figure 7. The areal proportion of each vegetation type with the distance to road. (The green solid line represents the areal proportion and the red dashed line represents average elevation within each road distance interval).

5. Discussion

5.1. Fine Classification of Vegetation Types Based on High-Resolution Remotely Sensed Data

Compared to traditional field surveys, combining remote sensing and GIS techniques can help better understand the vertical spatial patterns of vegetation distribution in mountainous areas. Previous studies have generally described the altitudinal spectrum in WNP as a transition from evergreen broadleaf forest to mixed coniferous and broadleaf forest, coniferous forest, elfin wood, and alpine meadows [36]. However, these studies lack detailed descriptions of the spatial distribution of specific tree species and the elevation ranges of transitional zones between different distribution belts. In this study, we refined the vertical distribution of vegetation types in WNP from low to high elevation and introduced compound transitional zone groups between various vertical zones (e.g., adding a low-altitude compound transitional zone before the dominant belt of broadleaf forest, including species such as Chinese fir), which enables an accurate description of the transition relationships between different vegetation types across vertical zones. High spatial resolution remote sensing data have the potential to provide fine classification results of vegetation types [41,42].

The diversity and complexity of mountainous vegetation types pose challenges for traditional vegetation mapping based on medium- or low-resolution remote sensing data [43]. The fine-grained features offered by high-resolution data have improved the issue of mixed pixels caused by heterogeneity among vegetation types. This enables the extraction of major vegetation types in mountainous areas and allows for a detailed characterization of their vertical distribution characteristics [44]. However, the vertical distribution patterns of vegetation types in mountainous areas based on remote sensing vegetation mapping results often rely on low-resolution classification products, which generally have only a very limited number of categories and reduce the applicability of analyzing the vertical differentiation patterns of complex mountainous vegetation landscapes [45]. This study identified some important tree species, such as Masson pine and Chinese fir, as well as farmland and tea plantation, by integrating Sentinel-2 and GF-6 data. It contributes to a better understanding of the vertical distribution patterns of vegetation types in mountainous areas. The PA and UA of Masson pine and Chinese fir are all greater than 70%. Furthermore, the classification accuracies of broadleaf forest, bamboo forest, and other types are higher than or comparable to those reported in previous studies [46–48]. We did not further subdivide broadleaf forest in this study, which limited the analysis of vegetation vertical differentiation patterns. The limited number of samples for different tree species and the capability of high-resolution multispectral data to identify tree species are key limiting factors for achieving fine-scale tree species recognition. With the advancement of satellite and airborne hyperspectral remote sensing, as well as the availability of a large number of tree species training samples and high-resolution DEM obtained from near-surface remote sensing such as an unmanned aerial vehicle (UAV), it becomes possible to achieve finer-scale tree species classification [49–51].

5.2. Vertical Characteristics of Vegetation Distribution in Wuyishan National Park

By leveraging the advantages of remote sensing technology in achieving spatially realistic analysis and combining the concept of "space-for-time substitution" commonly used in ecology, the spatial differences in the vertical distribution of vegetation types can provide insights into forest dynamics [52,53]. For example, the distribution peak of mixed coniferous and broadleaf forest at lower elevations indicates the change trend from Masson pine and Chinese fir to mixed coniferous and broadleaf forest [54]. Additionally, the similarities in vertical distribution (upper and lower limits and main distribution belts) between bamboo forest and broadleaf forest provide evidence for the competitive relationship between two vegetation types [55,56]. This study provided a detailed characterization of the vegetation altitudinal spectrum in WNP. Previous studies indicated that tree lines in different regions have been shifting upwards due to the influence of climate change and land-use changes caused by human activities [57–59]. Comparing the vertical distribution of major tree species in the 1980s [36], the upper limits of major tree species except bamboo forest in WNP have risen, with an elevation range of approximately 300–500 m (Table 7). This is larger than a previous study that reported the tree line moving upward by about 100 m due to increased average temperatures in WNP [34]. Considering the advantages of remote sensing technologies in obtaining vegetation types over field surveys, more research is needed to validate the vertical gradient changes. Bamboo forest did not show a significant change in the vertical distribution range. It might be due to insensitivity to the increased temperature, because the potential distribution of bamboo forest in China showed a tendency to contract inland and expand southwestward [60], and also decreased in northern China and other regions [61,62].

Table 7. Comparison of vertical distribution ranges of major forest types with historical data.

Vegetation Type	1980s (m) [36]	2019 (This Study)	
		Distribution Upper Limit/ Lower Limit (m)	Main Distribution Zone (m)
Masson pine	200–1100	200–1450	200–500
Chinese fir	500–1400	200–1950	200–600
Other coniferous forests	Southern hemlock 1500–1800 Huangshan pine 1200–1900	1300–2150	1300–1750
Mixed coniferous and broadleaf forest	500–1700	200–1950	200–1400
Broadleaf forest	350–1400	200–1950	200–1000
Bamboo forest	200–2158	200–2000	200–1050

5.3. Influences of Human Activities on Vertical Distribution of Vegetation Types

The vertical distribution of vegetation types in five different protection-level subregions reflects the roles of human activities and highlights the horizontal distribution patterns from the periphery to interior of the national park. Specifically, the areal proportions of vegetation types related to human activities (such as Chinese fir and tea plantation) show a decreasing trend along the horizontal gradient from the outer to the inner areas of the national park. This horizontal gradient of human disturbance-induced changes also contributes to the differences in vertical distribution patterns among different regions. For example, the scenic area exhibits more pronounced variations in the vertical distribution of vegetation types than the ecological and natural protection areas. Fan et al. [33] found that conservation measures effectively preserved the initial spatial pattern of vegetation coverage in WNP. Muise et al. [63] proved significant differences in forest structural attributes (such as height, coverage, and biomass) between protected and unprotected areas in the network of protected areas in British Columbia, Canada. However, we still know very little about the vertical distribution change patterns in these complicated mountainous ecosystems. The gradient and zonal changes of vegetation types along the periphery to the interior of WNP highlight the unique research value of examining the effects of zoning and hierarchical conservation management on the distribution of vegetation types in the national park.

The various change trends of vegetation types with road distance partially indicate that their distribution is influenced by human factors. Historically, considering the value of bamboo in timber, textiles, and food, some studies have found that human activities influence the spatial distribution of bamboo forest, leading to the so-called "invasion phenomenon" [64,65]. Our study found that bamboo forests are more distributed along the roadsides from Tongmu in the north to Guanping and in the south to Huangkeng (Figure 1c). These bamboo forests appear near the foothills along roads and residential areas and show the transition to broadleaf forest or mixed coniferous and broadleaf forest as elevation increases. However, it should be noted that bamboo forest exhibited a consistent distribution pattern as broadleaf and did not show significant changes along the distance from roads. It suggests that bamboo forest are not significantly affected by human influences, because they may have formed as a stable vegetation community type following the early destruction of existing broadleaf or coniferous forests. The differences in the areal proportions of vegetation types along road distance may have distinct underlying causes. Due to the multifaceted drivers of spatial distribution in vegetation types, the gradient changes may not be solely influenced by a single factor such as elevation or human factors. Within nature reserves, these influences may result from past large-scale afforestation activities and the current strict management measures [66,67]. For example, the similar changes trend between Masson pine and Chinese fir can be attributed to the fact that both are heavily influenced by human activities and exhibit close spatial proximity to each other (Figure 5). In addition, the areal proportions of mixed coniferous and broadleaf forest, other coniferous forests, and shrubland with the road distances showed similar change trends to elevation, indicating that there were similar factors influencing the change patterns of the horizontal gradient. The comprehensive analysis of road distance and DEM data reveals a similar trend of increasing elevation and then decreasing along the road distance, indicating that elevation factors partially influence the areal proportional distribution of each type along the road distance. This suggests that there may be a certain degree of relationship between the observed vertical distribution characteristics and the distribution patterns influenced by human activities. Separating the effects between these factors is one of the future research goals to deepen our understanding.

6. Conclusions

This research employed a modified hierarchy-based classifier based on the fused high-resolution remotely sensed data to produce the spatial distribution of vegetation types and then examined vertical characteristics of vegetation distributions in WNP. Our results show that (1) the classification results accurately depict the vegetation distribution, with an overall accuracy of 87.11% and Kappa coefficient of 0.85. The forests account for 91% of the total area in this park, with broadleaf forest, mixed coniferous and broadleaf forest, and bamboo forest being the predominant types; (2) Vegetation types show significant differences in vertical distribution with defined four compound dominant zone groups and five dominant belts; (3) There are variations in the areal proportions and vertical distribution characteristics of vegetation types in different subregions. The vegetation composition in the scenic area differs significantly from other subregions. The frequency of vertical distribution differences also varies among different vegetation types, with non-vegetated areas exhibiting the highest frequency of significant differences. The proportions of various vegetation types change with the distance from the road, and there are variations among different types (except for two pairs of types). The proportions of Masson pine and Chinese fir show a noticeable decreasing trend, while the changes in broadleaf forest and bamboo forest are less pronounced. This study presents a new means and perspective for understanding vertical vegetation distributions in a typical mountainous ecosystem, which will have positive implications for future environmental management in national parks or protected zones.

Author Contributions: Conceptualization, D.L. (Dengqiu Li) and D.L. (Dengsheng Lu); methodology, Y.Y., D.L. (Dengqiu Li) and D.L. (Dengsheng Lu); software, Y.Y. and D.L. (Dengqiu Li); validation, Y.Y., Z.W., K.L., M.Z., K.J. and D.L. (Dengqiu Li); formal analysis, Y.Y.; investigation, Y.Y., Z.W., K.L., M.Z., K.J. and D.L. (Dengqiu Li); resources, Y.Y., K.L., D.L. (Dengqiu Li) and D.L. (Dengsheng Lu); data curation, Y.Y.; writing—original draft preparation, Y.Y., D.L. (Dengqiu Li) and D.L. (Dengsheng Lu); writing—review and editing, Y.Y., D.L. (Dengqiu Li) and D.L. (Dengsheng Lu); visualization, Y.Y.; supervision, D.L. (Dengqiu Li) and D.L. (Dengsheng Lu); project administration, D.L. (Dengqiu Li) and D.L. (Dengsheng Lu); funding acquisition, D.L. (Dengqiu Li) and D.L. (Dengsheng Lu). All authors have read and agreed to the published version of the manuscript.

Funding: This research was financially supported by the Natural Science Foundation of Fujian Province, grant number 2022J01640 and 2022J011076, the National Natural Science Foundation of China, grant number 32371865, and public welfare projects of Fujian Provincial Science and Technology Department, grant number 2021R1002008.

Data Availability Statement: The data presented in this study are available on request from the corresponding author.

Acknowledgments: The authors thank reviewers for their help in improving our manuscript and thank Dan Zhuang for her help in difference significance test.

Conflicts of Interest: The authors declare no conflict of interest.

References

1. Körner, C. The use of 'altitude' in ecological research. *Trends Ecol. Evol.* **2007**, *22*, 569–574. [CrossRef]
2. Rahbek, C. The elevational gradient of species richness: A uniform pattern? *Ecography* **1995**, *18*, 200–205. [CrossRef]
3. Pompa-García, M.; González-Cásares, M.; Gazol, A.; Camarero, J.J. Run to the hills: Forest growth responsiveness to drought increased at higher elevation during the late 20th century. *Sci. Total Environ.* **2021**, *772*, 145286. [CrossRef] [PubMed]
4. Galván, J.D.; Camarero, J.J.; Gutiérrez, E. Seeing the trees for the forest: Drivers of individual growth responses to climate in Pinus uncinata mountain forests. *J. Ecol.* **2014**, *102*, 1244–1257. [CrossRef]
5. Beniston, M. Climatic change in mountain regions: A review of possible impacts. *Clim. Chang.* **2003**, *59*, 5–31. [CrossRef]
6. Zhao, F.; Zhang, B.; Zhu, L.; Yao, Y.; Cui, Y.; Liu, J. Spectra structures of altitudinal belts and their significance for determining the boundary between warm temperate and subtropical zones in the Qinling-Daba Mountains. *Acta Geogr. Sin.* **2019**, *74*, 889–901. [CrossRef]
7. Piiroinen, R.; Fassnacht, F.E.; Heiskanen, J.; Maeda, E.; Mack, B.; Pellikka, P. Invasive tree species detection in the Eastern Arc Mountains biodiversity hotspot using one class classification. *Remote Sens. Environ.* **2018**, *218*, 119–131. [CrossRef]
8. Zhang, Y.; Wu, X.; Zheng, D. Vertical differentiation of land cover in the central Himalayas. *J. Geogr. Sci.* **2020**, *30*, 969–987. [CrossRef]
9. Chen, W.; Ding, H.; Li, J.; Chen, K.; Wang, H. Alpine treelines as ecological indicators of global climate change: Who has studied? What has been studied? *Ecol. Inform.* **2022**, *70*, 101691. [CrossRef]

10. Gao, M.; Piao, S.; Chen, A.; Yang, H.; Liu, Q.; Fu, Y.H.; Janssens, I.A. Divergent changes in the elevational gradient of vegetation activities over the last 30 years. *Nat. Commun.* **2019**, *10*, 2970. [CrossRef]
11. Chen, Y.; Zhao, S.; Xie, Z.; Lu, D.; Chen, E. Mapping multiple tree species classes using a hierarchical procedure with optimized node variables and thresholds based on high spatial resolution satellite data. *GIScience Remote Sens.* **2020**, *57*, 526–542. [CrossRef]
12. Gómez, C.; White, J.C.; Wulder, M.A. Optical remotely sensed time series data for land cover classification: A review. *ISPRS J. Photogramm. Remote Sens.* **2016**, *116*, 55–72. [CrossRef]
13. Neigh, C.S.R.; Masek, J.G.; Bourget, P.; Rishmawi, K.; Zhao, F.; Huang, C.; Cook, B.D.; Nelson, R.F. Regional rates of young US forest growth estimated from annual Landsat disturbance history and IKONOS stereo imagery. *Remote Sens. Environ.* **2016**, *173*, 282–293. [CrossRef]
14. Kussul, N.; Lavreniuk, M.; Skakun, S.; Shelestov, A. Deep learning classification of land cover and crop types using remote sensing data. *IEEE Geosci. Remote Sens. Lett.* **2017**, *14*, 778–782. [CrossRef]
15. Fu, D.; Li, D.; Lu, D.; Chen, Y. Accuracy assessment of three 30 m resolution global land cover products in Fujian province based on survey data. *J. Fujian Norm. Univ.* **2023**, *39*, 122–136.
16. Tong, X.-Y.; Xia, G.-S.; Lu, Q.; Shen, H.; Li, S.; You, S.; Zhang, L. Land-cover classification with high-resolution remote sensing images using transferable deep models. *Remote Sens. Environ.* **2020**, *237*, 111322. [CrossRef]
17. Chen, Y.; Peng, Z.; Ye, Y.; Jiang, X.; Lu, D.; Chen, E. Exploring a uniform procedure to map Eucalyptus plantations based on fused medium–high spatial resolution satellite images. *Int. J. Appl. Earth Obs. Geoinf.* **2021**, *103*, 102462. [CrossRef]
18. Yu, X.; Lu, D.; Jiang, X.; Li, G.; Chen, Y.; Li, D.; Chen, E. Examining the roles of spectral, spatial, and topographic features in improving land-cover and forest classifications in a subtropical region. *Remote Sens.* **2020**, *12*, 2907. [CrossRef]
19. Blaschke, T.; Hay, G.J.; Kelly, M.; Lang, S.; Hofmann, P.; Addink, E.; Feitosa, R.Q.; Van der Meer, F.; Van der Werff, H.; Van Coillie, F. Geographic object-based image analysis–towards a new paradigm. *ISPRS J. Photogramm. Remote Sens.* **2014**, *87*, 180–191. [CrossRef]
20. Zhang, C.; Sargent, I.; Pan, X.; Li, H.; Gardiner, A.; Hare, J.; Atkinson, P.M. An object-based convolutional neural network (OCNN) for urban land use classification. *Remote Sens. Environ.* **2018**, *216*, 57–70. [CrossRef]
21. Estoque, R.C.; Murayama, Y.; Akiyama, C.M. Pixel-based and object-based classifications using high-and medium-spatial-resolution imageries in the urban and suburban landscapes. *Geocarto Int.* **2015**, *30*, 1113–1129. [CrossRef]
22. Vizzari, M. PlanetScope, Sentinel-2, and Sentinel-1 data integration for object-based land cover classification in Google Earth Engine. *Remote Sens.* **2022**, *14*, 2628. [CrossRef]
23. Hughes, G. On the mean accuracy of statistical pattern recognizers. *IEEE Trans. Inf. Theory* **1968**, *14*, 55–63. [CrossRef]
24. Lu, D.; Weng, Q. A survey of image classification methods and techniques for improving classification performance. *Int. J. Remote Sens.* **2007**, *28*, 823–870. [CrossRef]
25. Xie, Z.; Chen, Y.; Lu, D.; Li, G.; Chen, E. Classification of land cover, forest, and tree species classes with ZiYuan-3 multispectral and stereo data. *Remote Sens.* **2019**, *11*, 164. [CrossRef]
26. Belgiu, M.; Drăguţ, L. Random forest in remote sensing: A review of applications and future directions. *ISPRS J. Photogramm. Remote Sens.* **2016**, *114*, 24–31. [CrossRef]
27. Maxwell, A.E.; Warner, T.A.; Fang, F. Implementation of machine-learning classification in remote sensing: An applied review. *Int. J. Remote Sens.* **2018**, *39*, 2784–2817. [CrossRef]
28. Song, L.; Estes, A.B.; Estes, L.D. A super-ensemble approach to map land cover types with high resolution over data-sparse African savanna landscapes. *Int. J. Appl. Earth Obs. Geoinf.* **2023**, *116*, 103152. [CrossRef]
29. Ding, H.; Yang, Y.; Xu, H.; Fang, Y.; Chen, X.; Yang, Q.; Yi, X.; Xu, H.; Wen, X.; Xu, X. Species composition and community structure of the typical evergreen broad-leaved forest in the Wuyi Mountains of Southeastern China. *Acta Ecol. Sin.* **2015**, *35*, 1142–1154. [CrossRef]
30. Lan, S. Plant species diversity in Wuyishan national nature reserve. *Sci. Silvae Sin.* **2003**, *39*, 36–43. [CrossRef]
31. Guo, Y.; Lei, P.; Yan, Y.; Yuan, R.; Wu, S.; Li, J. Plant species diversity changes along altitudinal gradient on the northwest slope of Huanggang Mountain of Jiangxi Wuyi Mountain. *Chin. J. Ecol.* **2015**, *34*, 3002–3008. [CrossRef]
32. You, W.; He, D.; Huang, D.; Hong, W.; Wu, L.; Wang, Y.; Chen, B.; Yu, J.; Jiang, X. Spatial pattern and driving mechanism in Wuyishan scenery district. *Mt. Res.* **2011**, *29*, 677–687. [CrossRef]
33. Fan, M.; Liao, K.; Lu, D.; Li, D. Examining vegetation change and associated spatial patterns in Wuyishan National Park at different protection levels. *Remote Sens.* **2022**, *14*, 1712. [CrossRef]
34. Xu, D.; Geng, Q.; Jin, C.; Xu, Z.; Xu, X. Tree line identification and dynamics under climate change in Wuyishan National Park based on Landsat Images. *Remote Sens.* **2020**, *12*, 2890. [CrossRef]
35. Zhou, M.; Li, D.; Liao, K.; Lu, D. Integration of Landsat time-series vegetation indices improves consistency of change detection. *Int. J. Digit. Earth* **2023**, *16*, 1276–1299. [CrossRef]
36. He, J.; Lan, S.; Liu, C.; Li, L. Wuyishan research series. In *Natural Resources*; Xiamen University Press: Xiamen, China, 1994; ISBN 7-5615-0909-X.
37. Brodu, N. Super-resolving multiresolution images with band-independent geometry of multispectral pixels. *IEEE Trans. Geosci. Remote Sens.* **2017**, *55*, 4610–4617. [CrossRef]
38. Laben, C.A.; Brower, B.V. Process for Enhancing the Spatial Resolution of Multispectral Imagery Using Pan-Sharpening. U.S. Patent 6,011,875, 4 January 2000.

39. Myint, S.W.; Gober, P.; Brazel, A.; Grossman-Clarke, S.; Weng, Q. Per-pixel vs. object-based classification of urban land cover extraction using high spatial resolution imagery. *Remote Sens. Environ.* **2011**, *115*, 1145–1161. [CrossRef]
40. Jiang, X.; Zhao, S.; Chen, Y.; Lu, D. Exploring tree species classification in subtropical regions with a modified hierarchy-based classifier using high spatial resolution multisensor Data. *J. Remote Sens.* **2022**, *2022*, 9847835. [CrossRef]
41. Räsänen, A.; Virtanen, T. Data and resolution requirements in mapping vegetation in spatially heterogeneous landscapes. *Remote Sens. Environ.* **2019**, *230*, 111207. [CrossRef]
42. Zhao, S.; Jiang, X.; Li, G.; Chen, Y.; Lu, D. Integration of ZiYuan-3 multispectral and stereo imagery for mapping urban vegetation using the hierarchy-based classifier. *Int. J. Appl. Earth Obs. Geoinf.* **2021**, *105*, 102594. [CrossRef]
43. Jiang, H.; Chen, A.; Wu, Y.; Zhang, C.; Chi, Z.; Li, M.; Wang, X. Vegetation monitoring for mountainous regions using a new integrated topographic correction (ITC) of the SCS + C correction and the shadow-eliminated vegetation index. *Remote Sens.* **2022**, *14*, 3073. [CrossRef]
44. Wu, T.; Luo, J.; Gao, L.; Sun, Y.; Dong, W.; Zhou, Y.N.; Liu, W.; Hu, X.; Xi, J.; Wang, C.; et al. Geo-object-based vegetation mapping via machine learning methods with an intelligent sample collection scheme: A case study of Taibai Mountain, China. *Remote Sens.* **2021**, *13*, 249. [CrossRef]
45. Mao, X.; Deng, Y.; Zhu, L.; Yao, Y. Hierarchical geographic object-based vegetation type extraction based on multi-source remote sensing data. *Forests* **2020**, *11*, 1271. [CrossRef]
46. Du, H.; Mao, F.; Li, X.; Zhou, G.; Xu, X.; Han, N.; Sun, S.; Gao, G.; Cui, L.; Li, Y. Mapping global bamboo forest distribution using multisource remote sensing data. *IEEE J. Sel. Top. Appl. Earth Obs. Remote Sens.* **2018**, *11*, 1458–1471. [CrossRef]
47. Lu, M.; Chen, B.; Liao, X.; Yue, T.; Yue, H.; Ren, S.; Li, X.; Nie, Z.; Xu, B. Forest types classification based on multi-source data fusion. *Remote Sens.* **2017**, *9*, 1153. [CrossRef]
48. Zhou, G.; Ni, Z.; Zhao, Y.; Luan, J. Identification of bamboo species based on Extreme Gradient Boosting (XGBoost) using Zhuhai-1 orbita hyperspectral remote sensing imagery. *Sensors* **2022**, *22*, 5434. [CrossRef]
49. Michałowska, M.; Rapiński, J. A review of tree species classification based on airborne LiDAR data and applied classifiers. *Remote Sens.* **2021**, *13*, 353. [CrossRef]
50. Mäyrä, J.; Keski-Saari, S.; Kivinen, S.; Tanhuanpää, T.; Hurskainen, P.; Kullberg, P.; Poikolainen, L.; Viinikka, A.; Tuominen, S.; Kumpula, T. Tree species classification from airborne hyperspectral and LiDAR data using 3D convolutional neural networks. *Remote Sens. Environ.* **2021**, *256*, 112322. [CrossRef]
51. Ma, L.; Hurtt, G.; Tang, H.; Lamb, R.; Lister, A.; Chini, L.; Dubayah, R.; Armston, J.; Campbell, E.; Duncanson, L. Spatial heterogeneity of global forest aboveground carbon stocks and fluxes constrained by spaceborne lidar data and mechanistic modeling. *Glob. Change Biol.* **2023**, *29*, 3378–3394. [CrossRef]
52. Chraibi, E.; Arnold, H.; Luque, S.; Deacon, A.; Magurran, A.E.; Féret, J.-B. A remote sensing approach to understanding patterns of secondary succession in tropical forest. *Remote Sens.* **2021**, *13*, 2148. [CrossRef]
53. Lechner, A.M.; Foody, G.M.; Boyd, D.S. Applications in remote sensing to forest ecology and management. *One Earth* **2020**, *2*, 405–412. [CrossRef]
54. Zhang, W.; Chen, H.; Lin, W.; Dong, J.; Chen, S.; Zhao, W. Analysis on community diversity in coniferous-broadleaved mixed forests in Wuyi Mountain. *J. For. Environ.* **2016**, *36*, 136–140. [CrossRef]
55. Zhang, H.; Xue, J. Spatial Pattern and competitive relationships of Moso bamboo in a native subtropical rainforest community. *Forests* **2018**, *9*, 774. [CrossRef]
56. Yan, Y.; Xia, M.; Fan, S.; Zhan, M.; Guan, F. Detecting the competition between Moso bamboos and broad-leaved trees in mixed forests using a terrestrial laser scanner. *Forests* **2018**, *9*, 520. [CrossRef]
57. Chen, Y.; Lu, D.; Luo, G.; Huang, J. Detection of vegetation abundance change in the alpine tree line using multitemporal Landsat Thematic Mapper imagery. *Int. J. Remote Sens.* **2015**, *36*, 4683–4701. [CrossRef]
58. Ameztegui, A.; Coll, L.; Brotons, L.; Ninot, J.M. Land-use legacies rather than climate change are driving the recent upward shift of the mountain tree line in the Pyrenees. *Glob. Ecol. Biogeogr.* **2016**, *25*, 263–273. [CrossRef]
59. Jacob, M.; Frankl, A.; Beeckman, H.; Mesfin, G.; Hendrickx, M.; Guyassa, E.; Nyssen, J. North Ethiopian afro-alpine tree line dynamics and forest-cover change since the early 20th century. *Land Degrad. Dev.* **2015**, *26*, 654–664. [CrossRef]
60. Li, X.; Mao, F.; Du, H.; Zhou, G.; Xing, L.; Liu, T.; Han, N.; Liu, Y.; Zheng, J.; Dong, L. Spatiotemporal evolution and impacts of climate change on bamboo distribution in China. *J. Environ. Manag.* **2019**, *248*, 109265. [CrossRef]
61. Li, R.; Xu, M.; Wong, M.H.G.; Qiu, S.; Sheng, Q.; Li, X.; Song, Z. Climate change-induced decline in bamboo habitats and species diversity: Implications for giant panda conservation. *Divers. Distrib.* **2015**, *21*, 379–391. [CrossRef]
62. Tuanmu, M.-N.; Viña, A.; Winkler, J.A.; Li, Y.; Xu, W.; Ouyang, Z.; Liu, J. Climate-change impacts on understorey bamboo species and giant pandas in China's Qinling Mountains. *Nat. Clim. Chang.* **2013**, *3*, 249–253. [CrossRef]
63. Muise, E.R.; Coops, N.C.; Hermosilla, T.; Ban, S.S. Assessing representation of remote sensing derived forest structure and land cover across a network of protected areas. *Ecol. Appl.* **2022**, *32*, e2603. [CrossRef]
64. Liu, K.; Wang, A.; Zhang, S.; Zhu, Z.; Bi, Y.; Wang, Y.; Du, X. Tree species diversity mapping using UAS-based digital aerial photogrammetry point clouds and multispectral imageries in a subtropical forest invaded by Moso bamboo (*Phyllostachys edulis*). *Int. J. Appl. Earth Obs. Geoinf.* **2021**, *104*, 102587. [CrossRef]
65. Canavan, S.; Richardson, D.M.; Visser, V.; Le Roux, J.J.; Vorontsova, M.S.; Wilson, J.R. The global distribution of bamboos: Assessing correlates of introduction and invasion. *AoB Plants* **2017**, *9*, plw078. [CrossRef]

66. Ren, B.; Park, K.; Shrestha, A.; Yang, J.; McHale, M.; Bai, W.; Wang, G. Impact of human disturbances on the spatial heterogeneity of landscape fragmentation in Qilian Mountain national park, China. *Land* **2022**, *11*, 2087. [CrossRef]
67. Yang, H.; Viña, A.; Winkler, J.A.; Chung, M.G.; Dou, Y.; Wang, F.; Zhang, J.; Tang, Y.; Connor, T.; Zhao, Z.; et al. Effectiveness of China's protected areas in reducing deforestation. *Environ. Sci. Pollut. Res.* **2019**, *26*, 18651–18661. [CrossRef] [PubMed]